Digital Waveguide Modeling of Air-Driven Reed Generators for the Synthesis of Brass and Woodwind Instrument Sounds

GARY P. SCAVONE

Center for Computer Research in Music and Acoustics (CCRMA)
Department of Music, Stanford University
Stanford, California 94305 USA
gary@ccrma.stanford.edu

Abstract

This paper reviews past digital waveguide methods for reproducing non-linear "reed" excitations as well as introducing a new method incorporating reed dynamics. This model is based on a mass-spring-damper system and a non-linear flow control mechanism. In this way, a more physical system is attained which provides better approximations to the control parameters of real musical instruments. Further, it is shown that this model of the reed can be modified to represent the lips of a brass player, and the similarities and differences between these two systems are briefly examined.

1 Introduction

Musical instruments are most clearly distinguished from one another by their transient characteristics, which in turn are defined by a particular method of excitation. Among wind-blown instruments, for example, the various air-driven excitation methods distinguish saxophones from trumpets or flutes. In the context of digital waveguide modeling of musical instruments, highly accurate models of these non-linear excitation methods have proven difficult to produce. Two effective digital waveguide reed woodwind excitation methods have previously been presented (Smith 1986) (Cook 1992), though these models lack the *physical* control parameters associated with their real world counterparts. A dynamic waveguide reed model incorporating a mass-spring-damper system and non-linear flow control is presented here. The modeling of the reed in this way for waveguide applications was previously discussed in (Hirschman 1991) for woodwinds and (Cook 1991*b*) for brasses, though the flow control mechanisms implemented were different from that discussed in this paper.

2 Acoustical Aspects of Air-Driven Reed Generators

The acoustical properties of reed generators have been extensively studied (see Fletcher & Rossing 1991 for references). Two distinct types of reed generators exist those in which the reed valve is initially closed and then blown open (as with a brass player's lips) and those in which the reed valve is initially open and then blown closed (as for clarinets and saxophones). In most cases, the reed itself is modeled as a linear oscillator, and the pressure on the reed is taken equal to the difference in oral cavity and bore pressures. The position of the reed in turn governs the volume flow through the reed aperture, for which Bernoulli's flow equation forms a first approximation. Possible modifications to the flow equation include terms to compensate for reed channel inertia and the physical motion of the reed surface. Recent fluid-dynamic studies of flow through a reed aperture have suggested the need to account for viscous flow (Hirschberg et al. 1990). Non-linearity of the reed stiffness has also been discussed (Gilbert et al. 1990).

In woodwind instruments the reed resonance is normally high compared to the operating frequency of the reed. A mass-spring system driven at a frequency well below resonance is said to be stiffness dominated and its displacement amplitude will approach f/k, where k is the spring constant and f is the applied force. Thus, a common simplification for woodwind instruments has been to neglect the effect of the mass altogether and to simply model the reed system as a memory-less non-linearity. Assuming

the force on the reed is equal to $A \cdot p_\Delta$, where p_Δ is the difference in oral cavity and bore pressures and A is the approximate surface area of the reed exposed to p_Δ, the displacement of the reed from its equilibrium position (x_0) is given by Hooke's Law

$$x = \frac{A \cdot p_\Delta}{k} + x_0. \tag{1}$$

The area of the reed aperture is assumed to be proportional to x. Bernoulli's equation for steady volume flow through the reed aperture gives $u = \gamma |x| p_\Delta^{1/2}$, where γ is a constant dependent on the density of air and the area of the reed aperture. Combining this expression and Eq. (1), the volume flow is

$$u = \gamma \left| \frac{A p_\Delta^{3/2}}{k} + x_0 p_\Delta^{1/2} \right|. \tag{2}$$

Figure 1 displays the non-linear volume flow characteristic given by Eq. (2). An initial increase of p_Δ from zero results in a rapid increase in u. However, a continued increase of p_Δ begins to force the reed toward the mouthpiece lay, resulting in a decrease in volume flow. When $p_\Delta = p_{closure}$, the reed valve is completely closed.

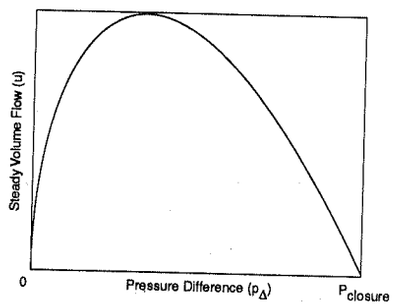

Figure 1: *Steady Flow Through a Pressure Controlled Valve Blown Closed*

3 Digital Waveguide Reed Generator Models

3.1 The Pressure Dependent Reflection Coefficient

McIntyre, Schumacher, & Woodhouse (1983) discussed the time-domain synthesis of clarinet sounds and incorporated a non-linear volume flow characteristic similar to that of Figure 1. Their procedure assumed continuity of volume velocity at the reed/bore junction and involved the simultaneous solution of a linear equation relating pressure to volume flow in the bore and a nonlinear approximation to Eq. (2), which related pressure to volume flow through the reed. As an efficient alternative to this process within the context of digital waveguide modeling, Smith (1986) proposed modeling the reed/bore boundary with a reflection coefficient that varies in response to the difference in oral cavity (p_{oc}) and bore pressures (p_b). The essential non-linear behavior of the reed is attained using an extremely simple calculation, though "higher order" reed behavior is sacrificed.

The pressure dependent reflection coefficient is derived by assuming continuity of volume velocity at the reed/bore junction,

$$\frac{p_\Delta}{Z_{oc}(p_\Delta)} = \frac{p_b^+ - p_b^-}{Z_b}, \qquad p_\Delta \triangleq p_{oc} - \left[p_b^+ + p_b^-\right] \tag{3}$$

and defining the reflection coefficient

$$\rho(p_\Delta) \triangleq \frac{1 + r(p_\Delta)}{1 - r(p_\Delta)}, \qquad r(p_\Delta) \triangleq \frac{Z_b}{Z_m(p_\Delta)}$$

Eq. (3) can then be solved for the reflected bore pressure at the junction, p_b^-

$$p_b^- = \rho(p_\Delta)p_b^+ + \frac{1-\rho(p_\Delta)}{2}p_{oc}. \tag{4}$$

Unfortunately, p_Δ is dependent on p_b^- and in order to solve Eq. (4) it is necessary to find an approximation to p_Δ. In a recursive, discrete-time calculation, it is possible to approximate $p_\Delta(n)$ by $p_\Delta(n-1)$ or to calculate $p_\Delta(n)$ using $p_b^-(n-1)$. Further, current values of either quantity could be extrapolated from previous values. The approach taken here is to define a new term, $p_\Delta^+ = p_{oc} - 2p_b^+$, which is independent of p_b^- and substitute this into Eq. (4) to obtain

$$p_b^- = \frac{p_{oc}}{2} - \rho(p_\Delta^+)\frac{p_\Delta^+}{2}. \tag{5}$$

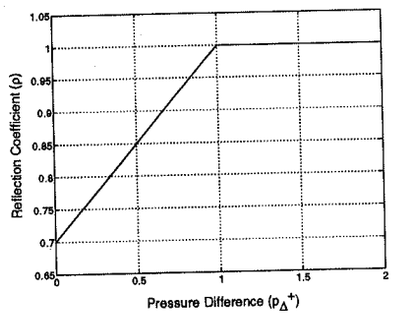

Figure 2: *Sample Reflection Coefficient Table*

The pressure dependent reflection coefficient is normally implemented using a look-up table, thereby saving one multiply and one addition per sample. Figure 2 displays a sample reflection coefficient table that has been used in synthesizing clarinet sounds. This particular table is based on normalized oral cavity pressure. Values of p_Δ^+ greater than 1.0 correspond to beating of the reed against the mouthpiece lay and complete reflection of incoming bore pressure. Values of differential pressure less than 1.0 correspond to partial reflection of p_b^+ and partial transmission of p_{oc} into the bore.

3.2 The Reed Reflection Polynomial

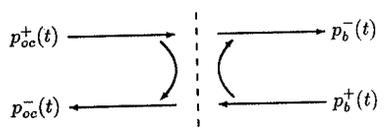

Figure 3: *Reed/Bore Scattering Junction*

The reed reflection polynomial incorporates the concept of a pressure dependent reflection coefficient but makes the assumption that p_Δ can be approximated by $p_{oc}^+ - p_b^+$. The polynomial model is derived by considering the reed/bore junction as shown in Figure 3. The portion of p_b^+ reflected back into the bore is given by $p_b^+ \cdot \rho(p_\Delta)$, while the portion of the oral cavity pressure which is transmitted into the bore is given by $p_{oc}^+(1-\rho(p_\Delta))$. Then p_b^- is given by

$$p_b^- = p_{oc}^+ - \left[p_{oc}^+ - p_b^+\right]\rho(p_\Delta). \tag{6}$$

Using the above stated approximation for p_Δ and approximating $\rho(p_\Delta)$ by a second order polynomial function, Eq. (6) becomes

$$p_b^- \approx p_{oc}^+ - \left[c_1(p_{oc}^+ - p_b^+) + c_2(p_{oc}^+ - p_b^+)^2 + c_3(p_{oc}^+ - p_b^+)^3\right]. \tag{7}$$

This reed implementation method has proven efficient and effective for real-time DSP synthesis. Unfortunately, the process of determining appropriate polynomial coefficients is rather arbitrary. It is possible to relate the polynomial coefficients to a polynomial approximation of the pressure dependent reflection coefficient through a matrix transformation (Cook 1991*a*).

3.3 The Dynamic Woodwind Reed Model

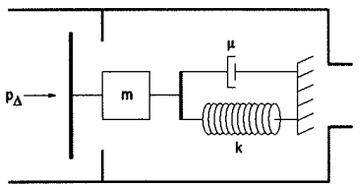

Figure 4: *Dynamic Woodwind Reed Model*

In contrast to the reed models previously discussed all of which ignored the mass of the reed the dynamic reed model seeks to accurately model the motion of the reed and its beating against the mouthpiece lay. In functioning as a pressure controlled valve, the position of the reed at any instant governs the volume flow that is injected at the reed/bore junction. The reed is represented by a linear mass-spring-damper system which is acted upon by the difference in oral cavity and bore pressures, as shown in Figure 4. The relationship between applied force and displacement, and the corresponding Laplace transform is given by

$$f_r(t) = m\frac{d^2x}{dt^2} + \mu\frac{dx}{dt} + kx \iff F_r(s) = \left[ms^2 + \mu s + k\right]X(s). \tag{8}$$

Both the oral-cavity and the bore pressures act upon the reed, so that the resultant force on the reed is

$$F_r(s) = A \cdot P_\Delta(s) = A \cdot [P_{oc}(s) - P_b(s)], \tag{9}$$

where A is the approximate surface area of the reed exposed to P_Δ. A is typically bounded by the width of the reed at its tip and the distance from the reed tip to the player's lower lip.

The transfer function that relates reed displacement to applied force is found from Eq. (8) as

$$\begin{aligned}\frac{X(s)}{F_r(s)} = H(s) &= \frac{1}{ms^2 + \mu s + k} \\ &= \frac{1/m}{s^2 + (\mu/m)\,s + \omega_o^2}\end{aligned} \tag{10}$$

where $\omega_o^2 = k/m$ is the natural frequency of the mass-spring system in the absence of damping. Using the bi-linear transform to convert from continuous to discrete time, the following digital transfer function results:

$$\begin{aligned}\frac{X(z)}{F_r(z)} = H(z) &= \frac{\left(1 + 2z^{-1} + z^{-2}\right)}{(k + \alpha^2 m + \alpha\mu) + 2\left(k - \alpha^2 m\right)z^{-1} + (k + \alpha^2 m - \alpha\mu)\,z^{-2}} \\ &= \frac{\left(1 + 2z^{-1} + z^{-2}\right)}{(m\omega_o^2 + \alpha^2 m + \alpha\mu) + 2m\left(\omega_o^2 - \alpha^2\right)z^{-1} + (m\omega_o^2 + \alpha^2 m - \alpha\mu)\,z^{-2}}\end{aligned} \tag{11}$$

where α is the bilinear transform constant used to control the frequency warping. The displacement found by passing $A \cdot p_\Delta(n)$ through this biquad section is subtracted from the reed's equilibrium position

(x_0) to produce the aperture spacing. Inelastic beating of the reed is assumed, such that the reed is forced against the lay and held there until the driving force decreases below $k \cdot x_0$, the force necessary to hold the spring stretched by x_0. The digital filter of Eq. (11) must be reset with the appropriate initial conditions each time this occurs. Figure 5 represents a transposed direct form II biquad filter structure that could be used to implement the reed filter. The appropriate internal state values to be used when the reed first begins to separate from the lay can be determined by inspection of the filter structure, given that the previous filter inputs and outputs are assumed to be $k \cdot x_0$ and x_0, respectively. In this case, the initializing values for the filter's internal states should equal $k \cdot x_0 \, (b1 + b2) - x_0 \, (a1 + a2)$ and $k \cdot x_0 \cdot b2 - x_0 \cdot a2$.

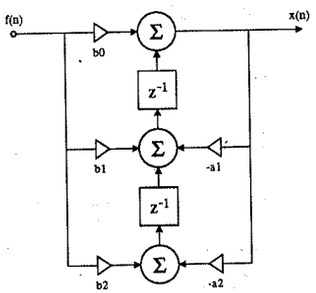

Figure 5: *Second Order Reed Filter*

Assuming that the Bernoulli flow equation applies to the given situation, the volume flow through the reed aperture is found from

$$\begin{aligned} u(t) &= A_r(t) \cdot v(t) \\ &= A_r(t) \cdot \left[\frac{2p_\Delta(t)}{\rho} \right]^{\frac{1}{2}} \end{aligned} \tag{12}$$

where $A_r(t) = w \cdot x(t)$ is the time-varying area of the reed aperture, w is the width of the reed, and ρ is the density of air.

Finally, we assume continuity of volume velocity at the reed/bore junction and calculate the new traveling wave component of pressure entering the bore as,

$$u(t) = u_b^+(t) + u_b^-(t) = \frac{p_b^+(t) - p_b^-(t)}{Z_b} \tag{13}$$

where $Z_b = \rho c / A_b$ is the constant acoustic characteristic impedance of the bore. $p_b^-(t)$ represents the traveling wave component of pressure entering the bore while $p_b^+(t)$ represents the traveling wave component of pressure leaving the bore. Solving for $p_b^-(t)$, we have

$$\begin{aligned} p_b^-(t) &= u(t) \cdot Z_b + p_b^+(t) \\ &= A_r(t) \cdot \left[\frac{2p_\Delta(t)}{\rho} \right]^{\frac{1}{2}} \cdot \frac{\rho c}{A_b} + p_b^+(t) \\ &= A_r(t) \cdot \frac{c}{A_b} \left[2\rho p_\Delta(t) \right]^{\frac{1}{2}} + p_b^+(t) \end{aligned} \tag{14}$$

Measurements on a clarinet reed and mouthpiece (Backus 1963) have shown the exponent value in Eq. (14) to be on the order of $\frac{2}{3}$. This calculation can be simplified for real-time DSP implementation by the use of a look-up table. In order to implement Eq. (14) in discrete-time, it is necessary to use an approximation to $p_\Delta(n)$ because of its dependence on $p_b^-(n)$. Given sufficiently high sampling rates and the fact that the bore oscillations are low-pass filtered by the bell/tonehole filter, a reasonable approximation that has produced acceptable results when implemented is $p_\Delta(n) = p_{oc}(n) - \left[p_b^+(n) + p_b^-(n-1) \right]$.

3.4 Modeling a Brass Player's Lips

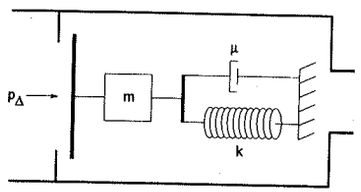

Figure 6: *Air-Driven Lip Model*

Figure 6 represents a basic air-driven lip model that can be used in brass instrument synthesis. In contrast to the woodwind reed model, this system is blown open and will oscillate near its resonance frequency. The derivation of Section 3.3 remains valid, though the lips do not beat against the mouthpiece. A similar model for brass instruments was developed in (Cook 1991*b*), though the discrete-time derivation and the flow control equations were different. In the woodwind model, frequency variation is principally controlled by adjustment of the resonator (delay-line) length, and the reed oscillations adjust appropriately. For the brass instrument model, however, both the acoustic resonator length and the lip model variables (mass, stiffness, and damping) control the sounding frequency. For a fixed resonator length corresponding to a fundamental frequency f_0, modification of the lip variables will cause the lip oscillations to become entrained at various partials of f_0. Likewise, holding the lip variables constant and varying the resonator length will result in a sounding frequency which fluctuates slightly about the resonance frequency of the lips. In essence, it is necessary that the lip resonance and the resonator length be modified in conjunction, as is required in the performance of real brass instruments. For these reasons, performance of waveguide brass instrument models is more difficult than for their woodwind counterparts and requires better control mechanisms.

4 Results & Future Refinements

The dynamic woodwind reed model presented here has been successfully implemented in digital waveguide woodwind instrument models and produces realistic transient and steady-state behaviors. Time-varying control of the reed parameters (mass, spring constant, and damping) is being explored. In particular, it is desired that the reed stiffness be variable over the course of the reed's motion. This is currently possible using three look-up tables for the filter coefficients, though more efficient methods for time-varying control are desired. The brass instrument model has been implemented only in *Matlab*, though similar real-time models by Perry R. Cook have previously been demonstrated. Current work is underway to implement all models in a real-time environment.

References

Backus, J. (1963). Small-vibration theory of the clarinet. *The Journal of the Acoustical Society of America*, 35(3), 305 313.

Cook, P. R. (1991*a*). Non-linear periodic prediction for on-line identification of oscillator characteristics in woodwind instruments. In (ICMC 1991), pp. 157 160.

Cook, P. R. (1991*b*). Tbone: An interactive waveguide brass instrument synthesis workbench for the NeXT machine. In (ICMC 1991), pp. 297 299.

Cook, P. R. (1992). A meta-wind-instrument physical model, and a meta-controller for real time performance control. In *Proceedings of the 1992 International Computer Music Conference*, pp. 273 276, San Jose, California.

Fletcher, N. H. & Rossing, T. D. (1991). *The Physics of Musical Instruments*. Springer-Verlag, New York.

Gilbert, J., Meynial, X., & Kergomard, J. (1990). The influence of the reed and the reed table on the fundamental frequency of a single-reed system. In *Journal de Physique II*, number C2 in Supplément au Journal de physique, pp. 833 836.

Hirschberg, A., Dane, H. J., Houtsma, A. J. M., Kruijswijk, S. G., van de Laar, R. W. A., Marrou-Maurières, J. P., & Wijnands, P. J. (1990). A quasi-stationary model of air flow in the reed channel of single-reed woodwind instruments. *Acustica*, 70(2), 146 154.

Hirschman, S. E. (1991). *Digital Waveguide Modeling and Simulation of Reed Woodwind Instruments*. Ph.D. thesis, Department of Electrical Engineering, Stanford University.

ICMC (1991). *Proceedings of the 1991 International Computer Music Conference*, Montreal, Canada.

McIntyre, M. E., Schumacher, R. T., & Woodhouse, J. (1983). On the oscillations of musical instruments. *The Journal of the Acoustical Society of America*, 74(5), 1325 1345.

Smith, J. O. (1986). Efficient simulation of the reed-bore and bow-string mechanisms. In *Proceedings of the 1986 International Computer Music Conference*, pp. 275 280, The Hague, Netherlands.

MUSICAL SCORE RECOGNITION OF "DON CUCO EL GUAPO" PIANIST ROBOT

A. Pedroza, H. Vargas, D. Vera and R. Fournier
Dept. of Microelectronics , Universidad Autónoma de Puebla
Boulevard Valsequillo y 14 sur A.P. J–32 Sn Manuel–72570
Puebla, Pue. México

Abstract

Don Cuco el Guapo is the first Mexican pianist robot, which was designed and built at the Departament of Microelectronics of the UAP. The project was based on multidisciplinary participation, where physicists, electronic engineers, computer scientists, musicians and designers converged.
The musical score recognition sytem was implemented through the following steps: frame grabbing, image processing, pattern recognition and interpretation or analysis of scene. The vision system of Don Cuco el Guapo is capable of reading musical score from a template.

Frame Grabbing

Frame grabbing is the process through which a visual image is taken from the three dimensional world. The frame grabbing involves different methods in order to reduce the graphic complexity, increasing the necessary information for object detection and extraction. These methods consist in the precise definition of the object to be captured, that is, what form characteristics does our object have so that the camera set up (focal distance, iris opening and focus) establishes a correspondence between the object (real image) and the plane image (digital image).

An ELECTRIM EDC−1000 camera was used for frame grabbing; it´s main characteristics include:

- CCD sensor
- High sensitivity
- Distorsionless image
- Fast response
- Resolution 192(h)x165(v)
- Monochromatic 8 bits
- Spectral range 400−1000 nm

Focal length was taken at one meter, with a variable iris for different illmination conditions. The visual information is converted to electric signal by the sensor CCD. When these signals are sampled and quantized, we obtain a digital image.